Published in final edited form as:

ChemNanoMat. 2016 May ; 2(5): 419–422. doi:10.1002/cnma.201500181.

Biomimetic Crystallization of $MnFe_2O_4$ Mediated by Peptide-Catalyzed Esterification at Low Temperature

Dr. Yoshiaki Maeda[a], **Dr. Zengyan Wei**[a], **Yasuhiro Ikezoe**[a], **Edmund Tam**[a], **Prof. Hiroshi Matsui**[a,b]

[a]Department of Chemistry and Biochemistry, City University of New York—Hunter College, 695 Park Ave., New York, NY 10065 (USA), hmatsui@hunter.cuny.edu

[b]Department of Biochemistry, Weill Medical College of Cornell University, 413 E. 69th Street, New York, NY 10021 (USA)

Abstract

Enzymes are some of the most efficient catalysts in nature. If small catalytic peptides mimic enzymes, there is potential for broad applications from catalysis for new material synthesis to drug development, due to the ease of molecular design. Recently a hydrogel-based combinatory phage display library was developed and protease-mimicking peptides were identified. Here we advanced the previous discovery to apply one of these catalytic peptides for the synthesis of bimetal oxide nanocrystals through the catalytic ester-elimination pathway. Conventional bimetal oxide crystallization usually requires high temperatures above several hundred °C; however, this catalytic peptide could grow superparamagnetic $MnFe_2O_4$ nanocrystals at 4°C. Superconducting quantum interference device (SQUID) analysis revealed that $MnFe_2O_4$ nano-crystals grown by the catalytic peptide exhibit superpara-magnetism. This study demonstrates the usefulness of protease-mimicking catalytic peptides in the field of material synthesis.

Keywords

biomineralization; catalytic peptide; ester elimination; $MnFe_2O_4$; superparamagnetism

Enzymes in nature are evolved efficiently to catalyze material growths in high yield and high selectivity at low temperature. Up to now, biomineralizing enzymes and peptides that catalyze the growth of metal nanocrystals have been isolated from tissues and cells of animals and microorganisms.[1] Recent comprehensive proteomic studies discovered metal-binding proteins that play critical roles in biomineralization.[2] For instance, the proteins derived from magnetotactic bacteria (e.g., Mms6)[2a] control the morphologies of magnetite crystals in the magnetosome organelles.[3] The biomineralization pathway starts from the uptake of metal precursors on metal-binding peptide sites, and then their catalytic properties nucleate and facilitate crystal growths. The biomineralization process is so efficient that crystals can be grown with low energy consumption (e.g., at low temperature). Thus far,

Supporting information for this article is available on the WWW under http://dx.doi.org/10.1002/cnma.201500181.

This manuscript is part of a Special Issue on Nanobiointerfaces. A link to the Table of Contents will appear here once the Special Issue is assembled.

several promising peptides or proteins can be used to catalyze the growth of inorganic nanomaterials.[4]

Recently, protease-mimicking CP4 peptides were used to catalyze ZnO nanocrystal formation through ester elimination.[5] Ester elimination favors the growth of metal oxides from metal acetate precursors through reverse hydrolysis of esters in organic environments, such as alcohols at high temperature.[6] The CP4 peptide was discovered from a combinatorial phage-display peptide library through a hydrogel-based biopanning process where phage viruses possessing protease-like activity can be purified by centrifugation due to product gel formation around peptides displayed at the tail of viruses.[5,7] Previously, this type of phage biopanning was also applied to identify peptides that can target cancer and stem cells.[8] The CP4 peptide is an efficient catalyst for metal oxide formation through the ester elimination pathway, and its amino acid residues (in particular, serine and lysine residues) could play an important role for crystallization.[5] While protease can catalyze the reverse hydrolysis of ester,[9] natural proteases are not ideal catalysts for metallization reactions because of the use of organic solvents. Small-peptide catalysts could have an advantage in catalyzing ZnO formation through ester elimination in organic solvents because organic-solvent-induced denaturing could be less problematic, as the conformation of the catalytic pocket of enzymes is more sensitive to the environment.[5]

Thus, the biomimetic approach is now recognized as a potential route to catalyze novel inorganic nanocrystal syntheses; however, most of these demonstrations were to grow simple noble metal or metal oxide nanocrystals, and the biosynthesis of bimetal oxide materials has not explored extensively.[10] In particular, spinel ferrites, MFe_2O_4 (M=Mn, Co, Zn, Ni, etc.), attracts high interest due to the great technological importance for electrode materials of Li-ion battery[11] as well as magnetic storage,[12] ferrofluids,[13] catalysts,[14] and biomedical applications.[15] The issue for the synthesis of spinel ferrites is that iron species could readily generate amorphous and low-crystallinity ferrihydrite at low temperature,[16] and thus there are few reports to mineralize the highly crystalline metal iron oxide below room temperature with biomolecular catalytic approaches.[17]

We hypothesize that this catalytic peptide-mediated ester elimination approach can be applicable for the synthesis of bimetal oxide materials at low temperature.[18] In a variety of bimetal oxides, $MnFe_2O_4$ is an interesting material for medical imaging and therapeutics in addition to magnetic storage.[19] Recently, $MnFe_2O_4$ nanocrystals were grown in a methanol (MeOH)–benzyl alcohol (BA) solvent system (50% volume ratio) with hydrothermal ester elimination.[20] In this study, the catalytic CP4 peptide was examined as to whether it can crystalize $MnFe_2O_4$ nanoparticles in the MeOH-BA system through the ester elimination pathway with no external energy inputs at low temperature. It was demonstrated that as-prepared $MnFe_2O_4$ nanocrystals consisted of single crystalline domains and these nanoparticles exhibited superparamagnetism, with a blocking temperature comparable with conventional $MnFe_2O_4$ nanoparticles synthesized with high-temperature treatments (100–3008C).

For the proposed catalytic $MnFe_2O_4$ nanocrystal growth, first the CP4 peptide (SMESLSKTHHYR, 1 $mgmL^{-1}$) and metal pre-cursors (50 mm manganese acetate

[$Mn(OAc)_2$] and 100 mm iron acetylacetonate [$Fe(AcAc)_3$]) were mixed in BA and MeOH in a 50% volume ratio. The formation of $MnFe_2O_4$ nanocrystals was observed, as shown in Figure 1a and 1b. $Mn(OAc)_2$ and $Fe(AcAc)_3$ provide Mn^{2+} and Fe^{3+} sources for the formation of manganese ferrite.[18] Selected area electron diffraction (SAED) confirms the formation of $MnFe_2O_4$ nanocrystals (inset of Figure 1a and Figure S1 in the Supporting Information). High-resolution TEM (HRTEM) imaging revealed that individual nanoparticles consisted of single crystalline domains and d-spacings of 5.000.71 and 3.17±0.14 Å were measured. These correspond to the {111} and {202} lattice fringes of $MnFe_2O_4$ (Figure 1b), further supporting the formation of target $MnFe_2O_4$. The as-prepared nanocrystals had a narrow size distribution of 5.9±1.2 nm in diameter (Figure 1c). EDX analysis of nanocrystals also supports the growth of $MnFe_2O_4$ with the catalytic peptide (Figure 1-d). In the absence of CP4, no crystal growth was observed (data not shown), thus demonstrating that the CP4 peptide is necessary for catalytic $MnFe_2O_4$ crystallization at low temperature.

To support the hypothesis that the crystallization of $MnFe_2O_4$ goes through the ester-elimination pathway, we looked for a by-product of methyl acetate from the esterification of acetate ion and alcohol.[6a] After the reaction mixtures were stirred with decane to dissolve nonpolar methyl acetate in the decane phase, remaining polar acetate and metal ions in the alcohol phase could be separated. When these by-products in the decane phase are analyzed by gas-chromatography mass-spectroscopy (GC-MS), methyl acetate is detected (Figure 2). This analysis supports the hypothesis that the CP4 peptides crystallize $MnFe_2O_4$ nanoparticles by catalyzing the ester-elimination pathway. It should also be noted that 100% BA cannot be used because of low solubility of the $Mn(OAc)_2$ precursor (the detailed GC-MS procedure is described in the Supporting Information).

The magnetic properties of resulting $MnFe_2O_4$ nanocrystals such as blocking temperature (T_B), coercivity and saturation magnetization were studied by using superconducting quantum interference device (SQUID) magnetometry. As shown in Figure 3a, the T_B for the $MnFe_2O_4$ nanocrystals is 41 K. Zero-field-cooled (ZFC) and field-cooled (FC) curves are superimposed at temperatures above T_B, suggesting that $MnFe_2O_4$ nanocrystals become superparamagnetic in this temperature range. The blocking temperature in this study is comparable to that of conventional $MnFe_2O_4$ nanoparticles prepared at high temperature (100–3008C), which have a similar size distribution.[21] This result indicates that both $MnFe_2O_4$ nanoparticles have comparable energy barriers of the magnetic anisotropy. As compared to the ferrimagnetic bulk $MnFe_2O_4$, these superparamagnetic nanoparticles are beneficial for many applications such as drug delivery, hyperthermic treatments, and contrast agents for magnetic resonance imaging (MRI).[22] The magnetic field dependence of magnetization is displayed in Figure 3b. At 2 K, that is, a temperature lower than T_B, $MnFe_2O_4$ nanocrystals displayed ferrimagnetic behavior with a coercivity value of 150 Oe and a saturation moment (M_s) of 2.5 $emug^{-1}$. The saturation moment is an order of magnitude lower than that reported by other study,[19] which indicates that our sample could contain amorphous domains around crystalline nanoparticle domains.

In conclusion, $MnFe_2O_4$ crystallization was achieved at extremely low temperature through the ester elimination pathway catalyzed by the CP4 dodeca-peptide. It was demonstrated that

as-prepared nanocrystals exhibited superparamagnetic properties with SQUID analysis. The current study shows the potential to develop enzyme-mimicking oligo-peptide catalysts through environmental friendly synthesis for technologically important metal oxide materials.

Experimental Section

Catalytic-peptide, esterification-mediated $MnFe_2O_4$ growth

Manganese acetate [$Mn(OAc)_2$, 50 mm=17.3 mgmL^{-1}] and [$Fe(AcAc)_3$, 100 mm=70.6 mgmL^{-1}] were dissolved in a mixture of MeOH and benzyl alcohol (1:1 volume ratio) by sonication. The mixture was centrifuged (18000×*g*, 30 min), and the supernatant was used as precursor solution. CP4 peptide (SMESLSKTHHYR, 0.5 mg) was suspended in the precursor solution (500 μL), sonicated and stirred on a shaker for 3 days at 4°C. The resulting suspension was transferred to a new tube and centrifuged (18000×*g*, 30 min). The collected pellet was washed with methanol (500 μL) and water (500 μL) under sonication and centrifuged again. The collected pellet was suspended in water, and used for further experiments.

TEM and EDX analysis

For the TEM observation, a drop of the $MnFe_2O_4$ sample (4 μL) was applied on a carbon-coated copper TEM grid (Electron Microscopy Sciences, PA, USA) and dried. The sample was examined by TEM (JEOL 2100) at 200 kV and EDX. The obtained digital images were analyzed using ImageJ program.

SQUID measurement

The magnetic properties such as blocking temperature (T_B), coercivity, and saturation magnetization were studied by using superconducting quantum interference device (SQUID) magnetometry (Quantum Design, MPMS). The $MnFe_2O_4$ sample (0.7 mg) was used for measurement. The temperature sweep from 2 to 60 K was performed in applied field of 100 Oe under both zero-field-cooled (ZFC) and field-cooled (FC; on cooling) conditions. The value of T_B was determined by the peak position in the ZFC curve.

Supplementary Material

Refer to Web version on PubMed Central for supplementary material.

Acknowledgements

All works were supported by the National Institute on Minority Health and Health Disparities (NIMHD) of the National Institutes of Health (NIH) (MD007599). Y.M. and H.M. thank Dr. Natasha A. Chernova (Binghamton University, SUNY) for SQUID measurements. Y.M. thanks Japan Society for the Promotion of Science, and the International Training Program provided through Tokyo University of Agriculture and Technology. E.T. thanks David Warren (Weill Cornell Medical College) for assisting with GC-MS.

References

[1]. Sarikaya M, Tamerler C, Jen AK, Schulten K, Baneyx F, *Nat. Mater.* 2003, 2, 577–585. [PubMed: 12951599]

[2]. a)Arakaki A, Webb J, Matsunaga T, *J. Biol. Chem*. 2003, 278, 8745–8750; [PubMed: 12496282] b)Kroger N, Deutzmann R, Sumper M, Science 1999, 286, 1129–1132; [PubMed: 10550045] c)Matsunaga T, Nemoto M, Arakaki A, Tanaka M, Proteomics 2009, 9, 3341–3352; [PubMed: 19579222] d)Nemoto M, Maeda Y, Muto M, Tanaka M, Yoshino T, Mayama S, Tanaka T, *Mar. Genom*. 2014, 16, 39–44;e)Nemoto M, Wang Q, Li D, Pan S, Matsunaga T, Kisailus D, Proteomics 2012, 12, 2890–2894; [PubMed: 22833255] f)Shimizu K, Cha J, Stucky GD, Morse DE, Proc. Natl. Acad. Sci. USA 1998, 95, 6234–6238; [PubMed: 9600948] g)Tanaka M, Okamura Y, Arakaki A, Tanaka T, Takeyama H, Matsunaga T, Proteomics 2006, 6, 5234–5247. [PubMed: 16955514]

[3]. a)Arakaki A, Yamagishi A, Fukuyo A, Tanaka M, Matsunaga T, Mol. Microbiol 2014, 93, 554–567; [PubMed: 24961165] b)Tanaka M, Mazuyama E, Arakaki A, Matsunaga T, J. Biol. Chem 2011, 286, 6386–6392. [PubMed: 21169637]

[4]. a)de La Rica R, Matsui H, Chem. Soc. Rev 2010, 39, 3499–3509; [PubMed: 20596584] b)Wei Z, Maeda Y, Matsui H, *Angew. Chem. Int. Ed.* 2011, 50, 10585–10588; Angew. Chem. 2011, 123, 10773–10776;c)Wang F, Mao CB, Chem. Commun 2009, 1222–1224;d)Nanda N, Koder RL, Nat. Chem 2010, 2, 15–24. [PubMed: 21124375]

[5]. Maeda Y, Wei Z, Ikezoe Y, Matsui H, ChemNanoMat, 2015, 1, 319.

[6]. a)Du H, Yuan F, Huang S, Li J, Zhu Y, Chem. Lett 2004, 33, 770–771;b)Niederberger M, Garnweitner G, Pinna N, Neri G, Prog. Solid State Chem 2005, 33, 59–70.

[7]. Maeda Y, Javid N, Duncan K, Birchall L, Gibson KF, Cannon D, Kanetsuki Y, Knapp C, Tuttle T, Ulijn RV, Matsui H, J. Am. Chem. Soc. 2014, 136, 15893–15896. [PubMed: 25343575]

[8]. a)Ma K, Wang D-D, Lin Y, Wang J, Petrenko V, Mao CB, Adv. Funct. Mater 2013, 23, 1172–1181; [PubMed: 23885226] b)Abbineni G, Modall S, Safiejko-Mroczka B, Petrenko V, Mao CB, Mol. Pharm 2010, 7, 1629–1642. [PubMed: 20735141]

[9]. Koeller KM, Wong CH, Nature 2001, 409, 232–240. [PubMed: 11196651]

[10]. a)Iwahori K, Yoshizawa K, Muraoka M, Yamashita I, *Inorg. Chem*. 2005, 44, 6393–6400; [PubMed: 16124819] b)Nuraje N, Su K, Haboosheh A, Samson, Manning EP, Yang N, Matsui H, Adv. Mater 2006, 18, 807–811; [PubMed: 31031545] c)Reiss BD, Mao C, Solis DJ, Ryan KS, Thomson T, Belcher AM, Nano Lett. 2004, 4, 1127–1132;d)Yamashita I, Hayashi J, Hara M, Chem. Lett 2004, 33, 1158–1159.

[11]. a)Chu YQ, Fu ZW, Qin QZ, Electrochim. Acta 2004, 49, 4915–4921;b)Zhang D, Zhang X, Ni X, Song JM, Zheng H, Chem. Phys. Lett 2006, 426, 120–123.

[12]. Lee DK, Kim YH, Kang YS, Stroeve P, J. Phys. Chem. B 2005, 109, 14939–14944. [PubMed: 16852892]

[13]. a)Auzans E, Zins D, Blums E, Massart R, J. Mater. Sci 1999, 34, 1253– 1260;b)Tourinho FA, Franck R, Massart R, J. Mater. Sci 1990, 25, 3249–3254.

[14]. Kanazawa A, Kanaoka S, Yagita N, Oaki Y, Imai H, Oda M, Arakaki A, Matsunaga T, Aoshima S, *Chem. Commun*. 2012, 48, 10904–10906.

[15]. Lee JH, Huh YM, Jun YW, Seo JW, Jang JT, Song HT, Kim S, Cho EJ, Yoon HG, Suh JS, Cheon J, *Nat. Med*. 2007, 13, 95–99. [PubMed: 17187073]

[16]. a)Hashimoto H, Yokoyama S, Asaoka H, Kusano Y, Ikeda Y, Seno M, Takada J, Fujii T, Nakanishi M, Murakami R, J. Magn. Magn. Mater 2007, 310, 2405–2407;b)Sakai T, Miyazaki Y, Murakami A, Sakamoto N, Ema T, Hashimoto H, Furutani M, Nakanishi M, Fujii T, Takada J, Org. Biomol. Chem 2010, 8, 336–338. [PubMed: 20066267]

[17]. a)Staniland S, Williams W, Telling N, Van Der Laan G, Harrison A, Ward B, Nat. Nanotechnol 2008, 3, 158–162; [PubMed: 18654488] b)Tanaka M, Brown R, Hondow NS, Arakaki A, Matsunaga T, Staniland SS, *J. Mater. Chem*. 2012, 22, 11919–11921.

[18]. Bilecka I, Djerddj I, Niederberger M, *Chem. Commun*. 2008, 886–888.

[19]. a)Vestal CR, Zhang ZJ, *J. Am. Chem. Soc*. 2003, 125, 9828–9833; [PubMed: 12904049] b)Yang H, Zhang C, Shi X, Hu H, Du X, Fang Y, Ma Y, Wu H, Yang S, Biomaterials 2010, 31, 3667–3673; [PubMed: 20144480] c)Peng Y, Wang Z, Liu W, Zhang H, Zuo W, Tang H, Chen F, Wang B, *Dalton Trans*. 2015, 44, 12871–12877. [PubMed: 26102593]

[20]. a)Clavel G, Willinger MG, Zitoun D, Pinna N, *Adv. Funct. Mater*. 2007, 17, 3159–3169;b)Tonto P, Mekasuwandumrong O, Phatanasri S, Pavarajarn V, Praserthdam P, *Ceram. Int*. 2008, 34, 57–62;c)Pinna N, Niederberger M, Angew. Chem. Int. Ed 2008, 47, 5292–5304;

[21]. Vestal CR, Song Q, Zhang ZJ, *J. Phys. Chem. B* 2004, 108, 18222–18227.

[22]. a)Corr SA, Byrne SJ, Tekoriute R, Meledandri CJ, Brougham DF, Lynch M, Kerskens C, O'Dwyer L, Gun'ko YK, *J. Am. Chem. Soc*. 2008, 130, 4214–4215; [PubMed: 18331033] b)Kim KS, Park J-K, Lab Chip 2005, 5, 657–664; [PubMed: 15915258] c)Laurent S, Dutz S, Hfeli UO, Mahmoudi M, *Adv. Colloid Interface Sci*. 2011, 166, 8–23; [PubMed: 21601820] d)Motte L, Benyettou F, de Beaucorps C, Lecouvey M, Milesovic I, Lalatonne Y, *Faraday Discuss*. 2011, 149, 211–225. [PubMed: 21413183]

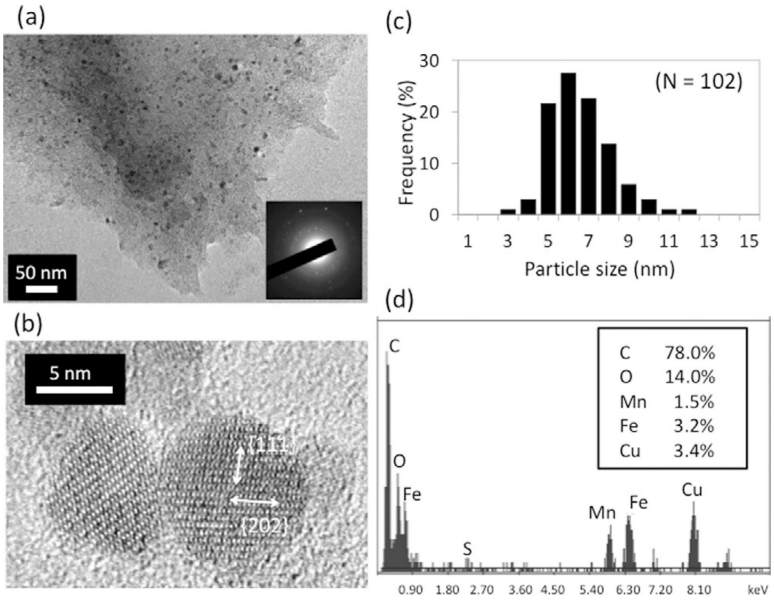

Figure 1.

Formation of $MnFe_2O_4$ nanocrystals with enzyme-mimicking CP4 peptide and Fe and Mn precursors in MeOH/BA at 4°C. (a) TEM image of $MnFe_2O_4$ nanocrystals (dark spots). SAED (inset) supports formation of $MnFe_2O_4$ (a facet-assigned pattern at higher magnification is shown in the Supporting Information). (b) $MnFe_2O_4$ nanocrystals are confirmed to be single crystalline by HRTEM observation. (c) The narrow size distribution of $MnFe_2O_4$ nanocrystals. (d) EDX analysis of a nanocrystal detects both manganese and iron.

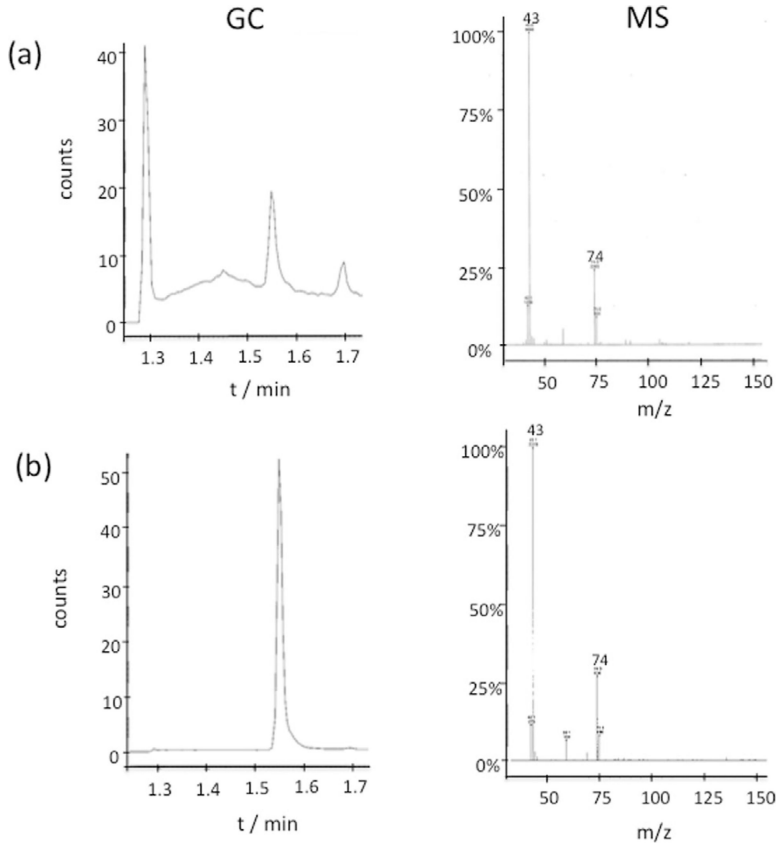

Figure 2.

GC-MS analysis of the by-product, methyl acetate, in the sample extracted from the supernatant after mixing $MnFe_2O_4$ growth precursors and CP4 peptide. (a) The sample from the supernatant, and (b) a standard methyl acetate. Molecular weight for methyl acetate is 74.08.

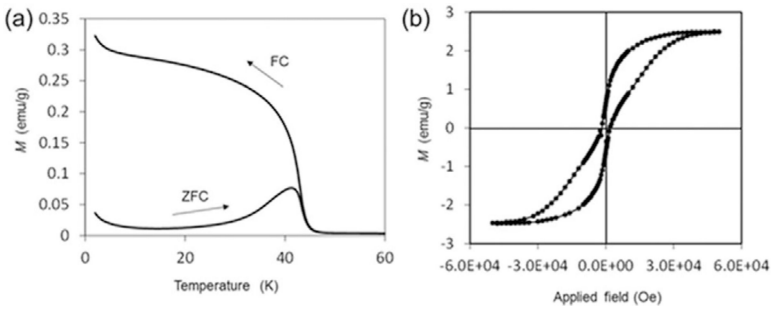

Figure 3.

SQUID studies for the $MnFe_2O_4$ nanocrystals prepared with the CP4 peptide in MeOH/BA. (a) ZFC and FC magnetizations of $MnFe_2O_4$ nanocrystals measured in applied field of 100 Oe. (b) Hysteresis loop measurement of $MnFe_2O_4$ nanocrystals at 2 K.